

Using Solid Phase Micro Extraction Method To Separate The Trace Elements From River Water Samples By Nano Graphene Oxide As A Sorbent

Safaa Sabri Najim^{1*}, Samara J. Mohammad² and Hawraa Hameed Rady³

Chemistry department, Collage of Science, Misan University- Iraq

Physics Department, College of Science for women, University of Baghdad-Iraq

Abstract

Water samples obtained from rivers in Maysan province, Iraq, were used to separate and determine trace components in river water. NGO was synthesized using a modified Hummer's method and characterized using a Fourier transform infrared spectrophotometer (FT-IR), ultraviolet-visible spectrophotometer (UV-Vis), X-ray diffraction spectroscopy (XRD), Zeta potential analyzer, Transmission electronic microscopy (TEM), and field emission scanning electronic microscopy (FESEM) (FESEM). The synthesized NGO was utilized to separate the trace elements (Cr, Fe, Cu, Zn, Cd, and Pb) from river water samples at optimal circumstances using the solid phase micro extraction technique (SPME). Cr, Fe, Cu, Zn, Cd, and Pb contents in river water samples (1.771 g/mL), (0.791 g/mL), (0.44 g/mL), (1.53 g/mL), (0.498 g/mL), and (1.345 g/mL) were evaluated directly by flame atomic absorption spectroscopy. Cr, Fe, Cu, Zn, Cd, and Pb had lower average residue concentrations after SPME utilizing nano sheets of GO as a sorbent (0.38 g/mL), (0.098 g/mL), (0.079 g/mL), (0.191 g/mL), (0.021 g/mL), and (0.191 g/mL), respectively. There was a shift in conductivity values in water samples evaluated before and after the addition of nano sheets of GO, confirming the adsorption of metal ions on the nano sheets of GO.

Key words: Trace elements, Solid phase micro extraction method. Nano graphene oxide, Conductivity.

1. Introduction

Heavy metal ions in water and soil produce "environmental pollution," which may be traced back to industrial expansion due to high pollution levels in rivers, lakes, and seas, resulting in heavy metal ion deposits⁽¹⁻³⁾. Arsenic, lead, mercury, chromium, zinc, cadmium, copper, and nickel are all heavy metals that cause pollution⁽⁴⁻⁵⁾. In recent years, graphene oxide has been studied as a possible material for metal ion adsorption^(6,7). GO having multiple oxygenation groups functionalized on the edge of sheets⁽⁸⁻¹²⁾. In GO, this functionalized group specifies a surface area and dispersion properties⁽¹⁾.

Graphene oxide has been extensively studied as a heavy metal ion adsorbent in aquatic environments due to its electrostatic interaction with cations. Heavy metal cations are attracted to negatively charged graphene oxide flakes by electrostatic forces, resulting in better sorption performance in aqueous solution⁽¹³⁾. Solid phase micro extraction (SPME) is a popular method for the separation and pre-concentration of metal ions, commonly used before atomic absorption spectrometry (AAS)⁽¹⁾, nano graphene oxide used as a sorbent in

solid phase micro extraction method SPME In this study synthesized nano graphene oxide used as a sorbent in order to separate and remove the trace elements at the optimum conditions from the river water by solid phase micro extraction method – SPME.

2. Methodology

2.1 Instruments

The operating conditions for FAAS are presented in Table-1. Flame atomic absorption spectroscopy (FAAS) AI-1200, the analytes (Cr, Fe, Cu, Zn, Cd, and Pb) were determined using Aurora. Spectrophotometer (UV-vis) (double beam, UV-1800, Shimadzu), Fourier transform infra-red (FTIR-8400S, Shimadzu), Zeta potential analyzer (ELS type, zeta plus, Brookhaven), X-ray diffraction (XRD, LabX-XRD-6000, Shimadzu), Field emission scanning electronic microscopy (FESEM, 5KV, Zeiss), Probe sonicator (FSFJY92-IIN, Sino Sonics), stirring water bath (KBLEE 2010) and Muffle furnace (CWF1100).

Table-1 Operating parameters of FAAS according to manual instructions

Elements	Wave length (nm)	Slit width (nm)	HCLamp (mA)	Calibration curve (µg/mL)	Flame
Cr	357.9	0.2	10	0.2 – 0.8	Air/acetylene
Fe	248.3	0.2	5	0.5 – 2.0	Air/acetylene
Cu	324.7	0.2	6	0.5 – 2.0	Air/acetylene
Zn	213.9	0.2	5	0.5 – 2.0	Air/acetylene
Cd	288.8	0.2	5	0.5 – 2.0	Air/acetylene
Pb	217.0	0.2	5	2.0 – 8.0	Air/acetylene

2.2 Chemicals

Standard solutions were prepared by serial dilution of stock solutions (1000 µg/mL) using deionized water (19.5 S/cm). Chromium chloride, Ferrous sulphate, Copper sulphate, Zinc sulphate, Cadmium sulphate and Lead nitrate from Sigma-Aldrich. Graphite (99.9 %) - CDH company, Sulphuric acid (97%), Hydrochloric acid (37%) – ChemLab, Dimethyl formamide (99.5%), Potassium permanganate, Sodium nitrate, Thomas Beaker, Hydrochloric acid (37%) AppliChem, Hydrogen peroxide (50%) Chem Lap.

2.3 Synthesis of nano graphene oxide

A modified Hummer's approach was used to synthesize nano graphene oxide (NGO)^(14,15). In beaker 500 mL dissolved 0.6 g graphite and 0.5 g sodium nitrate (NaNO₃) in 23 ml of cooled (0 °C) concentrated sulphuric acid (H₂SO₄) onto ice bath with stirring for 15 min. A added gradually 3.0 g potassium permanganate (KMnO₄) to the suspension (black color), continuous stirring to keep the reaction temperature below 20 °C onto ice bath for 30 min. Then stirring in water bath at 35 °C for 2hrs. (The suspension changed to dark brown). Deionized water 50 ml added gradually (by dropper) into the suspension over a hot plate magnetic stirrer, the temperature kept below 98 °C, for 15 min, warm deionized water 100 ml added. Hydrogen peroxide (30% H₂O₂) 10 ml added gradually (by dropper) to remove the residual KMnO₄ and MnO₂, for 15 min. The suspension separated by centrifuge (4000 rpm for 5 min), the precipitate washed with warm hydrochloric acid (HCl) 5% to remove sulphate ions, Then wash the solution in deionized water until pH 7. Dried the product (graphene oxide) in oven at 60 °C for 1 hr. Graphene oxide 0.5 g added to 50 ml of N,N-di methyl formamide (DMF) solvent and sonicated by probe sonicator for 30 min, the suspension separated by centrifuge (4000 rpm for 10 min), the separated residue dried in oven at 60 °C for 1 hr.

2.4 Solid phase micro extraction method (SPME) to separate analytes from samples

The analytes (Cr, Fe, Cu, Zn, Cd and Pb) determined directly in river water samples by FAAS. The optimum conditions of solid phase micro extraction method (SPME) by using nano graphene oxide sheets, 20 ml water sample volume, optimum pH for each analyte ion, NGO mass = 0.5 mg, sonicated time 2 min., stirring time 5 min. at room temperature and three droplets of 6.5 mg/mL NaCl, centrifuged for 5 min (5000 rpm) to separate the solid phase of NGO from the solution, analytes concentration determined in the residual solutions by FAAS⁽¹⁶⁾.

2.5 Conductivity

The presence and absence of nano graphene oxide sheets, the conductivity of river water samples collected from various parts of the Maysan governorate was examined. There was a change in conductivity values before and after the addition of nano graphene oxide sheets; the conductivity values were high before and reduced after the addition of nano graphene oxide sheets. This confirmed the separation of the trace elements from the river water samples as shown in Table-2.

Table-2 Conductivity values in the absence and presence of nano sheets of graphene oxide

Samples	G_{Ohm}^{-1}	G_{Ohm}^{-1}
	Absence NGO	Presence NGO
1	3.8×10^{-3}	2.0×10^{-4}
2	3.5×10^{-3}	5.6×10^{-4}
3	3.4×10^{-3}	1.5×10^{-4}
4	3.2×10^{-3}	1.3×10^{-4}
5	2.7×10^{-3}	1.7×10^{-4}
6	3.5×10^{-3}	1.6×10^{-4}
7	4.3×10^{-3}	1.8×10^{-4}
8	3.6×10^{-3}	1.3×10^{-4}
9	3.7×10^{-3}	1.6×10^{-4}
10	3.4×10^{-3}	1.0×10^{-4}

3. Results and discussion

3.1 NGO Characterization

The FT-IR spectra of synthesized NGO is shown in Fig. 1-a, with a band at 1626 cm^{-1} for the C=C bond and a wide band at 3360-3460 cm^{-1} for the OH bond. The C=O band stretching vibrations of carbonyl and carboxylic groups first observed at 1709 cm^{-1} , While the epoxy group stretching vibrations about 1217 cm^{-1} to COOH and 1035 cm^{-1} to CO. The maximum absorption peak, $\lambda_{max} = 239.5$ nm, and a shoulder peak, 289.5 nm, were the absorption bands that corresponded to poly aromatic C=C bonds to $\pi \rightarrow \pi^*$ electron transitions and $n \rightarrow \pi^*$ electron transitions of C=O bonds, respectively, in the UV-vis spectrum of the NGO dispersion (0.1 mg/mL), as shown in Fig. 1-b⁽¹⁷⁾. FT-IR and UV-vis spectra indicated the presence of multiple oxygen functional groups (hydroxyl, carboxyl, carbonyl, and epoxy groups) on the surface of the synthesized NGO. The zeta potential of synthesized NGO was (-17.17 mV), as shown in Fig. 1-c. Zeta potentials analyze the surface charge on a particle, which impacts nanomaterial agglomeration and adsorption of ions onto nano surface⁽¹⁸⁾. The XRD spectrum of graphite, $2\theta = 26.7^\circ$ ⁽¹⁹⁾, The oxidation process caused the peak to disappear, and a new peak appeared at a

lower angle ($2\theta \approx 11^\circ$), indicating the existence of the synthesized NGO, as shown in Fig. 1-d. The obtained results agree with the previous studies^(20,21). As shown in Fig. 1, a TEM image exhibiting the intensity of electrons attenuated by NGO platelets of various thicknesses shows a sheet-like morphology with different thicknesses (3-8). Dark spots represent the dense stacking nanostructure of many nano graphene oxide layers with distinct oxygen functional groups. As a result of stacking nanostructure exfoliation, the higher transparency areas imply significantly thinner nanographene oxide sheets with only a few layers. The obtained results agree with the previous studies^(22, 23). The FESEM used to study the surface morphology of NGO as shown in Fig. 2, the corrugation shape observed. Low wrinkled on NGO surface are more sensitive and show better adsorption ability⁽²⁴⁾. The energy dispersive X-ray (EDX) (attached with the FESEM), used to identify the elements involved in the NGO formation as shown in Fig. 2, the appearance of a peak at energy (0.18 keV) to carbon atoms, and another peak at energy (0.5 keV) to oxygen atoms, proved the presence carbon and oxygen atoms only in pure synthesized NGO. The obtained results agree very well with the previous studies^(15,25).

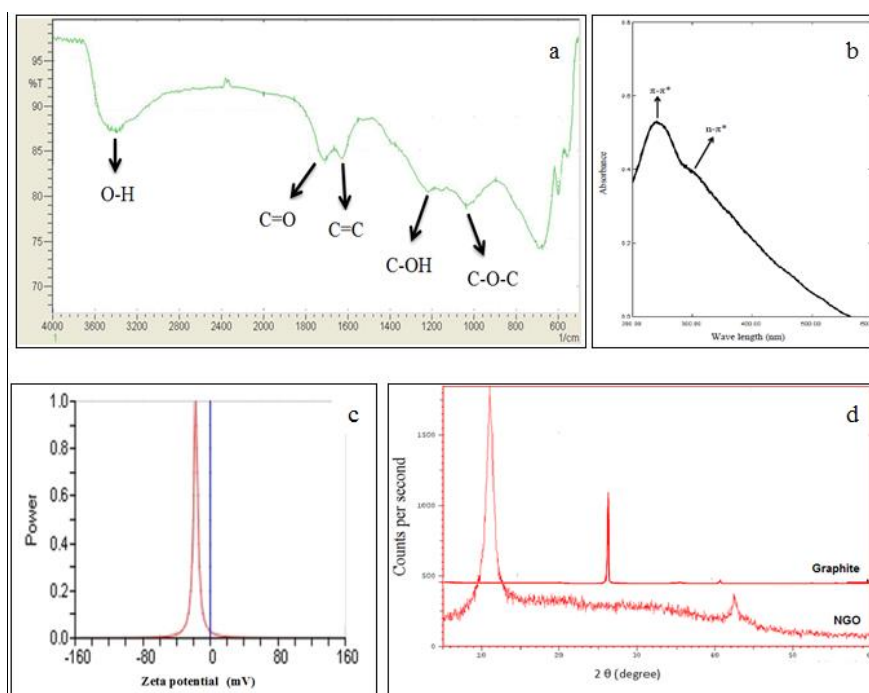


Fig. 1: Characterization of NGO synthesized (a) FT-IR, (b) UV-vis absorption spectrum, (c) Zeta potential, (d) XRD

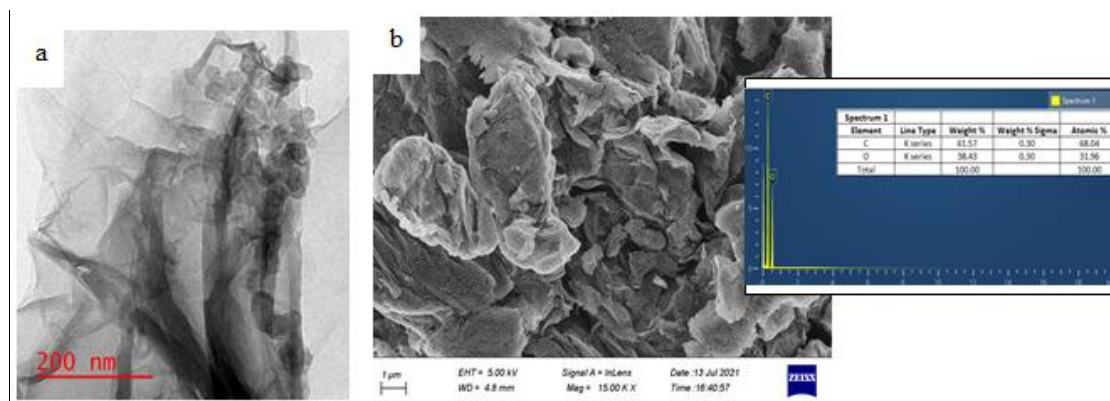


Fig. 2: (a) TEM image, (b) FESEM Image and EDX of the synthesized NGO

3.2 Optimization of solid phase micro extraction method (SPME)

The adsorption procedure for (Cr+3, Fe+2, Cu+2, Zn+2, Cd+2, and Pb+2) ions was carried out in this study utilizing the solid phase micro extraction (SPME) technique with nano graphene oxide, and the recovery determinete for the solution was studied using flame atomic absorption spectroscopy (FAAS).The recovery was evaluated by using the equation $R\% = [(C_{added} - C_{after}) / C_{added}] * 100\%$, where C_{added} the direct concentration of analytes (without NGO), and C_{after} the concentration of analytes by the SMPE method⁽⁴⁸⁾. The optimum pH for each analyte ion sufficiently for adsorption process on NGO sheets surface area as shown in Fig. (3-a). NGO mass, the recovery increased 0.25-1.0 mg as shown in Fig. (3-b), The obtained recovery 0.5 mg explained the availability of more sorption sites on NGO sheets surface⁽²⁶⁾.

The results show the recovery of the analyte ions remained constant within 20 – 50 mL of sample volumes, but less than 20 mL the recovery of metal ions decreased under optimum conditions because the adsorption capacity independent on the volume of sample ⁽²²⁾ show in the Figure (3-c). Stirring time (5-120 min) does not play a significant role in SPME method as shown in Fig. (3-d), results show Because the equilibrium of available sorption sites for metal ions was reached quickly, the adsorption process was highly speedy. The sonication time, remained constant in the range (2-10 min), while the recovery of the metal ions without sonicated was lower than 2 min., because the solution is not dispersed (accumulated), therefore, incomplete adsorption on surface of the NGO sheets as shown in Fig. (3-e).

With a change in temperature, the recovery of metal ions did not differ significantly., but at 70°C the recovery is decreased because of the weak electrostatic forces between the metal ions and the sheet surface charge of the NGO sheets at high temperatures (the process of adsorption is exothermic)⁽⁴⁹⁾ as shown in Fig. (3-f). As shown in Fig. 1, the effectiveness of adsorption rose considerably with increasing NaCl concentration (2 - 6.5 mg mL⁻¹) and decreased with increasing NaCl concentrations (7 - 8 mg mL⁻¹). Low NaCl concentrations (3 g) resulted in inefficient NGO aggregation and analyte adsorption. Owing to competition between positive sodium ions and analyte ions, higher NaCl concentrations resulted in considerable analyte elution from NGO, whereas lower NaCl concentrations resulted in significant analyte elution from NGO due to competition between positive sodium ions and analyte ions⁽²⁷⁾.

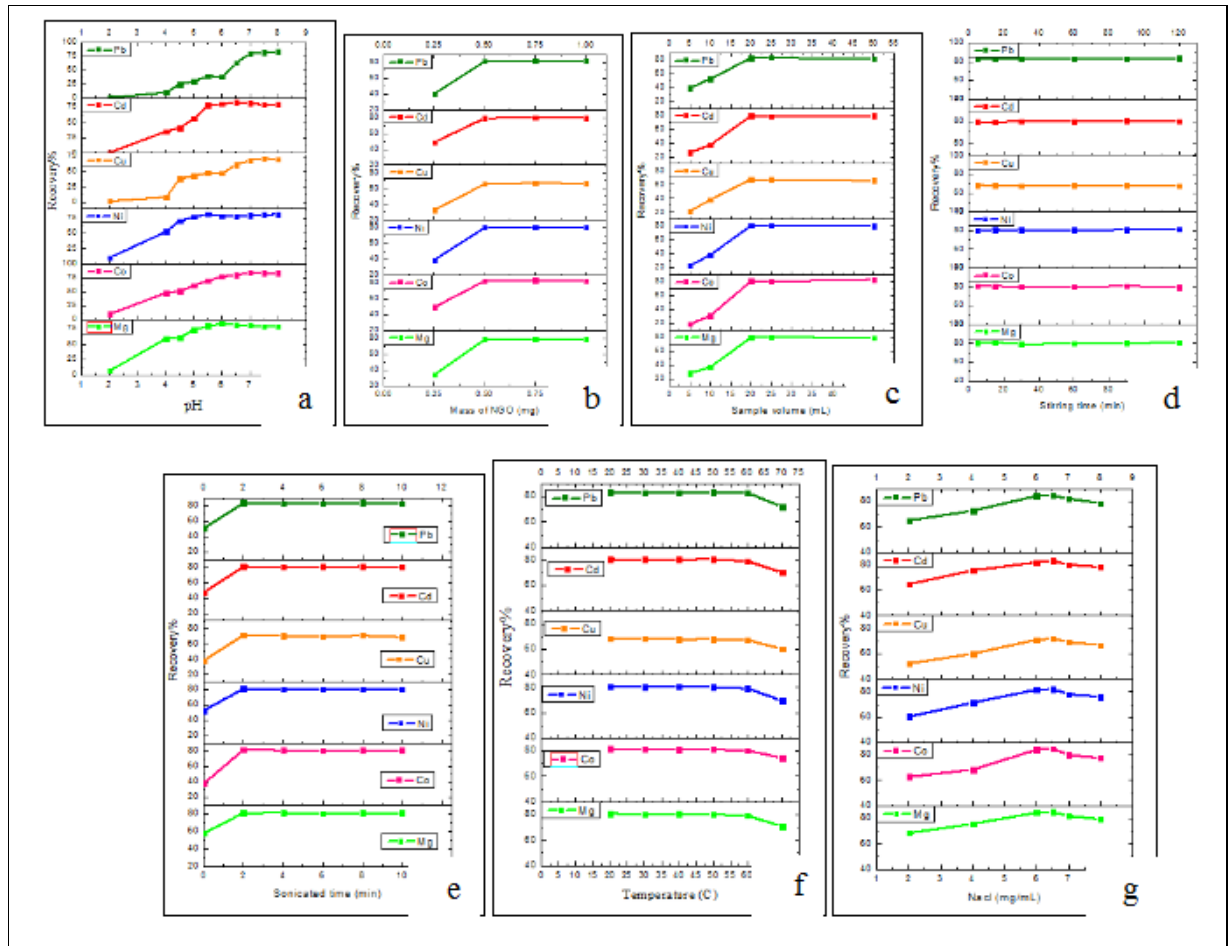


Fig. 3: Optimum conditions of SPME, (a) pH, (b) NGO mass, (c) Sample volume, (d) Stirring time, (e) Sonicated time, (f) Temperature, (g) NaCl Concentration

3.3 Adsorption capacity

The adsorption capacity of analytes calculated by using equation, $q (\mu\text{g}/\text{mg}) = \frac{(C_0 - C)V}{W}$ Where q is the amount of analyte adsorbed per unit weight of NGO, The starting and residual analyte concentrations are C_0 and C , respectively, the sample volume is V , and the NGO weight is W ⁽²²⁾. Adsorption capacity of Mg, Co, Ni, Cu, Cd and Pb ($1\mu\text{g}/\text{mL}$) calculated at optimum conditions of SPME method as shown in table-3.

Table 3: Adsorption Capacity of analyte ions

Analyte	Recovery %	Adsorption Capacity ($\mu\text{g}/\text{mg}$)
Cr	75.9	30.36
Fe	83.0	33.20
Cu	71.9	28.76
Zn	82.3	32.92
Cd	83.3	33.32
Pb	84.9	33.96

3.4 Analytical performance

Table 4 and Fig. 4 show the analytes measured directly by FAAS using the SPME technique under optimal circumstances. Because of the adsorption of the analyte metals ions on the surface of the NGO sheets, the concentrations of analytes in river water samples reduced utilizing the SPME technique.

Table 4: Concentration of analytes by direct and SPME method and recovery of river water samples

Samples	Analyte																	
	Cr			Fe			Cu			Zn			Cd			Pb		
	µg/mL		Recovery %	µg/mL		Recovery %	µg/mL		Recovery %	µg/mL		Recovery %	µg/mL		Recovery %	µg/mL		Recovery %
	Direct method	SPME method		Direct method	SPME method		Direct method	SPME method		Direct method	SPME method		Direct method	SPME method		Direct method	SPME method	
1	1.074	0.212	80.3	0.965	0.1332	86.2	0.374	0.045	88	1.321	0.1532	88.4	0.256	0.014	94.6	0.805	0.112	86.1
2	1.27	0.254	80	0.893	0.1214	86.4	0.146	0.016	89.3	1.46	0.181	87.6	0.421	0.011	97.3	1.288	0.193	85
3	1.456	0.296	79.7	0.713	0.087	87.8	0.121	0.013	89.6	1.36	0.1618	88.1	0.518	0.015	97.1	0.962	0.139	85.5
4	1.598	0.332	79.2	0.711	0.0846	88.1	0.178	0.019	89.1	2.244	0.3142	86	0.288	0.01	96.4	1.148	0.157	86.3
5	1.635	0.347	78.8	0.714	0.0814	88.6	0.216	0.025	88.3	1.669	0.2136	87.2	0.447	0.019	95.8	1.437	0.188	86.9
6	1.845	0.387	79	0.843	0.1087	87.1	0.226	0.028	87.7	1.148	0.1274	88.9	0.609	0.014	97.7	1.468	0.197	86.6
7	2.052	0.443	78.4	0.706	0.0755	89.3	0.647	0.118	81.8	1.061	0.1135	89.3	0.481	0.021	95.6	0.969	0.103	89.4
8	2.188	0.492	77.5	0.79	0.0956	87.9	0.658	0.129	80.4	2.104	0.284	86.5	0.424	0.017	96	1.07	0.146	86.4
9	2.253	0.502	77.7	0.794	0.0913	88.5	0.793	0.162	79.6	1.747	0.2271	87	0.821	0.07	91.5	1.168	0.167	85.7
10	2.336	0.535	77.1	0.778	0.1027	86.8	1.044	0.236	77.4	1.186	0.1364	88.5	0.713	0.016	97.7	3.132	0.504	83.9
RSD%	24.5	29.14		11.09	18.772		73.281	98.17		26.3912	35.311		35.45	84.38		49.239	60.23	

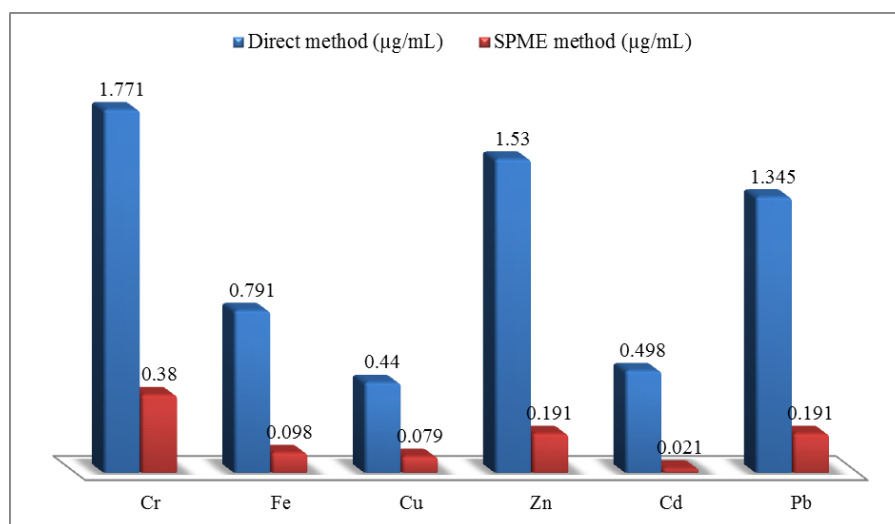


Fig. 4: Average concentration of analytes by direct and SPME methods in river water samples

Conclusions

Because of the presence of oxygen groups (anionic nature) on NGO sheets, analyte ions (cation nature) may be adsorbed fast and efficiently on the NGO surface. The suggested approach is cationic ion exchange chromatography, in which the NGO (anionic nature) functions as a stationary phase sorbent and the analyte solution (cationic nature) acts as a mobile phase, with no substantial changes in the analytes' adsorption ability. The cost, time efficiency, and economic consumption of just 0.5mg NGO as a sorbent are all advantages of this procedure.

Acknowledgment

The authors appreciated all the Lab. facilities of the chemistry department of College of science- Misan university.

References

1. Kong, Q.; Preis, S.; Li, L.; Luo, P.; Wei, C.; Li, Z.; Hu, Y.; Wei C. Relations between metal ion characteristics and adsorption performance of graphene oxide: A comprehensive experimental and theoretical study. *Sep Purif Technol.* 2020;(232):115956.
 2. Radu, V.M.; Ionescu, P.; Diacu, E.; Ivanov AAI. Removal of heavy metals from aquatic environments using water hyacinth and water lettuce. *Rev Chim.* 2017;(68):2765–2767.
 3. Kong, Q.; Li, Z.; Zhao, Y.; Wei, C.; Qiu, G.; Wei C. Investigation of the fate of heavy metals based on process regulation-chemical reaction-phase distribution in an A-O1-H-O2 biological coking wastewater treatment system. *J Environ Manag.* 2019;(247):234–241.
 4. Antoun, H.; Kloepper J. Plant Growth Promoting Rhizobacteria (PGPR). *Encycl Genet.* Published online 2001:1477–1480.
 5. Malik, L.A.; Bashir, A.; Qureashi, A.; Pandith A. Detection and removal of heavy metal ions. *A Rev Environ Chem Lett.* 2019;(17):1495–1521.
 6. Wang, X.; Chen, L.; Wang, L.; Fan, Q.; Pan, D.; Li, J.; Chi, F.; Xie, Y.; Yu, S.; Xiao C. et al. Synthesis of novel nanomaterials and their application in efficient removal of radionuclides. *Sci China Chem.* 2019;(62):933–967.
 7. Boukhvalov, D.W.; Katsnelson M. Modeling of graphite oxide. *J Am Chem Soc.* 2008;(130):10697–10701.
 8. Casabianca, L.B.; Shaibat, M.A.; Cai, W.W.; Park, S.; Piner, R.; Ruoff, R.S.; Ishii Y. NMR-based structural modeling of graphite oxide using multidimensional ¹³C solid-state NMR and ab initio chemical shift calculations. *J Am Chem Soc.* 2010;(132):5672–5676.
 9. Guerrero-Contreras, J.; Caballero-Briones F. Graphene oxide powders with different oxidation degree, prepared by synthesis variations of the Hummers method. *Mater Chem Phys.* 2015;(153):209–220.
 10. Figueiredo, J.L.; Pereira, M.F.R.; Freitas, M.M.A.; Órfão JJM. Modification of the surface chemistry of activated carbons. *Carbon N Y.* 1999;(37):1379–1389.
 11. Allahbakhsh, A.; Haghghi, A.; Sheydaei M. Poly(ethylene trisulfide)/graphene oxide nanocomposites. *J Therm Anal Calorim.* 2017;(128):427–442.
 12. Justh, N.; Berke, B.; László, K.; Szilágyi I. Thermal analysis of the improved Hummers' synthesis of graphene oxide. *J Therm Anal Calorim.* 2018;(131):2267–2272.
- and Naphthol on Reduced Graphene Oxide. *Environ. Sci Technol.* 2017;51:3278–3286.
13. Chen L, Shi G, Shen J, et al. Ion sieving in graphene oxide membranes via cationic control of interlayer spacing. *Nature.* 2017;550(7676):380-383. doi:10.1038/nature24044
 14. Chen J, Yao B, Li C, Shi G. An improved Hummers method for eco-friendly synthesis of graphene oxide. *Carbon N Y.* 2013;64(1):225-229. doi:10.1016/j.carbon.2013.07.055
 15. Zaaba NI, Foo KL, Hashim U, Tan SJ, Liu WW, Voon CH. Synthesis of Graphene Oxide using Modified Hummers Method: Solvent Influence. *Procedia Eng.* 2017;184:469-477.
 16. Ahmed Abd ulwahid Mohammed SSN and HHR. Using Solid Phase Micro Extraction Method to Separate The Trace Elements from Crude Oil Samples by Nano Graphene Oxide as a Sorbent. *Turkish J Physiother Rehabil.* 2021;32(3):23182-23191.
 17. Crouch S, Skoog D, Holler FJ. Principles of Instrumental Analysis Seventh Edition. Vol 88.; 2016.
 18. Varenne F, Coty JB, Botton J, et al. Evaluation of zeta potential of nanomaterials by electrophoretic light scattering: Fast field reversal versus Slow field reversal modes. *Talanta.* 2019;205(June):120062.
 19. Ain QT, Haq SH, Alshammari A, Al-Mutlaq MA, Anjum MN. The systemic effect of PEG-nGO-induced oxidative stress in vivo in a rodent model. *Beilstein J Nanotechnol.* 2019;10(April):901-911.
 20. Stobinski L, Lesiak B, Malolepszy A, et al. Graphene oxide and reduced graphene oxide studied by the XRD, TEM and electron spectroscopy methods. *J Electron Spectros Relat Phenomena.* 2014;195(March 2018):145-154.

21. Krishnamoorthy K, Veerapandian M, Yun K, Kim SJ. The chemical and structural analysis of graphene oxide with different degrees of oxidation. *Carbon* N Y. 2013;53:38-49.
22. Liou TH, Lin MH. Characterization of graphene oxide supported porous silica for effectively enhancing adsorption of dyes. *Sep Sci Technol*. 2020;55(3):431-443.
23. Drewniak S, Muzyka R, Stolarczyk A, Pustelny T, Kotyczka-Morańska M, Setkiewicz M. Studies of reduced graphene oxide and graphite oxide in the aspect of their possible application in gas sensors. *Sensors (Switzerland)*. 2016;16(1).
24. Xu Y, Nguyen Q, Malekahmadi O, et al. Synthesis and characterization of additive graphene oxide nanoparticles dispersed in water: Experimental and theoretical viscosity prediction of non-Newtonian nanofluid. *Math Methods Appl Sci*. 2020;(February):1-20.
25. Paquin F, Rivnay J, Salleo A, Stingelin N, Silva C. Multi-phase semicrystalline microstructures drive exciton dissociation in neat plastic semiconductors. *J Mater Chem C*. 2015;3(207890):10715-10722.
26. Atkins, P. W.; de Paula J. *Physical Chemistry* (8th ed.). Oxford Univ Press. Published online 2006:764.
27. Deng D, Jiang X, Yang L, Hou X, Zheng C. Organic solvent-free cloud point extraction-like methodology using aggregation of graphene oxide. *Anal Chem*. 2014;86(1):758-765.